NRC Trailer Skirts: SmartWay verification testing using the NRC 9 m Wind Tunnel: final report

Kirchhefer, Adam J.; McAuliffe, Brian R.

Publisher’s version / Version de l'éditeur:
https://doi.org/10.4224/40001933
Laboratory Technical Report (National Research Council of Canada. Aerospace. Aerodynamics Laboratory); no. LTR-AL-2016-0009-V4, 2016-11-16

NRC·CNRC

AERODYNAMICS LABORATORY

NRC Trailer Skirts - SmartWay Verification Testing using the NRC 9 m Wind Tunnel Final Report

Unclassified Unlimited

LTR-AL-2016-0009 -V4

November 16, 2016

Adam J. Kirchhefer and Brian R. McAuliffe

National Research Council Canada Conseil national de recherches Canada

Canada

AERODYNAMICS LABORATORY

NRC Trailer Skirts - SmartWay Verification Testing using the NRC 9 m Wind Tunnel Final Report

Report No.: LTR-AL-2016-0009 -V4

Date: November 16, 2016

Authors: Adam J. Kirchhefer and Brian R. McAuliffe

Classification:	Unclassified	**Distribution:**	Unlimited
For:	Fleet Forward 2020		
Project #:	A1-006030		
Submitted by:	Dr. Steven J. Zan, **Director R&D Aerodynamics**		
Approved by:	Jerzy Komorowski, **General Manager, Aerospace Portfolio**		

Pages:	46	**Copy No:**	-
Figures:	25	**Tables:**	5

Abstract

This report documents the procedure and results of a wind-tunnel-based SmartWay verification test program to evaluate the aerodynamic performance of the *NRC Trailer Skirts*. The testing was performed in the NRC 9 m Wind Tunnel using a 30%-scale model of a tractor-trailer combination. The NRC Trailer Skirts were measured to have a reduction in wind-averaged drag of 9.9% which is estimated to provide a fuel savings of 5.4±0.1%.

Table of Contents

List of Figures

List of Tables

Nomenclature

Symbols:

A	Frontal area of 30%-scale tractor-trailer model [m^2]
D	Drag force [N]
Δf	Reduction of fuel consumption [%]
$\delta\Delta f$	Uncertainty in the reduction of fuel consumption [%]
C_D	Drag coefficient [-]
$C_{D,W}$	Effective drag coefficient which includes resistance of wheel rotation [-]
I_{WIND}	Current supplied to wheel motors subjected to wind loads [Amp]
I_0	No-load current of wheel motors [Amp]
r	Wheel radius [m]
Q_C	Dynamic pressure in the test section corrected for blockage [Pa]
U_{avg}	Mean terrestrial wind speed [m/s]
U_g	Vehicle ground speed [m/s]
WAC_D	Wind-averaged coefficient of drag [-]
$\Delta WACd$	Change in wind-averaged coefficient of drag [-]
β	Vehicle-referenced wind angle [°]
ϵ	Uncertainty in the difference between two wind-averaged coefficients of drag
ρ	Density of air [kg/m^3]
θ	Terrestrial wind angle [°]
τ	Torque coefficient of the DC motors [Nm/Amp]

Acronyms:

BLCS	Boundary Layer Control System
EPA	Environmental Protection Agency
GESS	Ground Effect Simulation System
NRC	National Research Council Canada
RTS	Road Turbulence System

1. Introduction

The SmartWay program, developed by the U.S. Environmental Protection Agency (U.S. EPA), provides an opportunity for manufacturers of tractor or trailer fuel-saving devices to obtain verification of device performance from a third party. To obtain verification, a specific process must be followed by the manufacturer and approved by the U.S. EPA. Details of the SmartWay process for wind-tunnel testing are outlined by EPA (2015).

This is a final-report document, submitted to the EPA SmartWay program, to demonstrate the capability of the National Research Council Canada (NRC) of testing an aerodynamic device for SmartWay verification. Testing of the ***NRC Trailer Skirts*** was performed in the NRC 9 m Wind Tunnel using the NRC 30%-scale tractor-trailer model to demonstrate its applicability for SmartWay verification tests. A pre-test report was previously submitted for approval of the test-plan and approach (Kirchhefer and McAuliffe, 2015). This final report documents all relevant information from the pre-test report, including aspects of the test facility, test method, and data reduction used, and provides the test results.

2. Test Article

2.1 Tractor-Trailer Combination

The device tested in this report is evaluated based on its impact on the wind-averaged coefficient of drag of the NRC's 30% scale tractor-trailer combination, shown in Figures 2.1 and 2.2.

The 30%-scale tractor-trailer is a detailed wind tunnel model of a heavy duty vehicle (HDV), capable of adopting a range of configurations typical of full-scale HDVs on North American roads. The model can accommodate different gap sizes, cab styles, trailer types, and wheel sizes. Furthermore, the model is instrumented with pressure taps over many of its surfaces, and anemometers behind the front grille. For the purpose of SmartWay verification, the model has a sleeper-cab configuration based in-part on a current aero-tractor by popular manufacturer, with a tractor-trailer gap set to 1.14 m (45 in) full scale. The tractor is modelled after an International/Navistar ProStar with modifications made to the bumper, hood, A-pillars and roof fairing per Navistar's request. Care was taken to ensure that these modifications would not adversely affect the aerodynamic performance of the tractor in any significant manner. Based on NRC's vast experience with testing full-scale and model-scale heavy vehicles, the changes to the vehicle shape are not expected to adversely affect the vehicle's aerodynamic performance by any more than 2-3%, if at all. The tractor has the following aerodynamic components representative of SmartWay-designated tractors, also highlighted in Figure 2.1:

- Integrated sleeper cab roof fairing;
- Aerodynamic mirrors;
- Aerodynamic bumper;
- Tractor Gap Reducers (17 inch full-scale); and
- Fuel tank fairings.

Underbody structures (landing gear, mud flaps, etc.) are present with high fidelity (Figures 2.3 and 2.4). The model trailer is a full-scale equivalent of a 53 ft dry-van trailer with a tandem axle wheel setup. The aft trailer axle was positioned an equivalent 3.05 m (10 ft) from the base of the trailer, corresponding to the California Vehicle Code, section 35400(b)(4). The radius of the trailer's front edges is full-scale equivalent 0.15 m (6 in). The SmartWay-required test-article descriptions are provided in Table 2.1. All dimensions relevant to the test (*SAE Wind Tunnel Test Procedure for Trucks and Busses*, 2012) are shown in Figure 2.5 and listed in Table 2.6.

The model is supported by six streamlined struts. The six struts extend horizontally from the model; four from the lower edge of the trailer and two from the tractor. All struts connect to vertical streamlined columns which are connected to a balance underneath the wind tunnel floor. The support struts and internal structure of the model are sufficiently rigid not to deflect significantly under wind loads. Underneath the model, a moving belt simulates a moving

Figure 2.1: Photograph of NRC 30%-scale tractor-trailer model - front view.

Figure 2.2: Photographs of NRC 30%-scale tractor-trailer model - rear view.

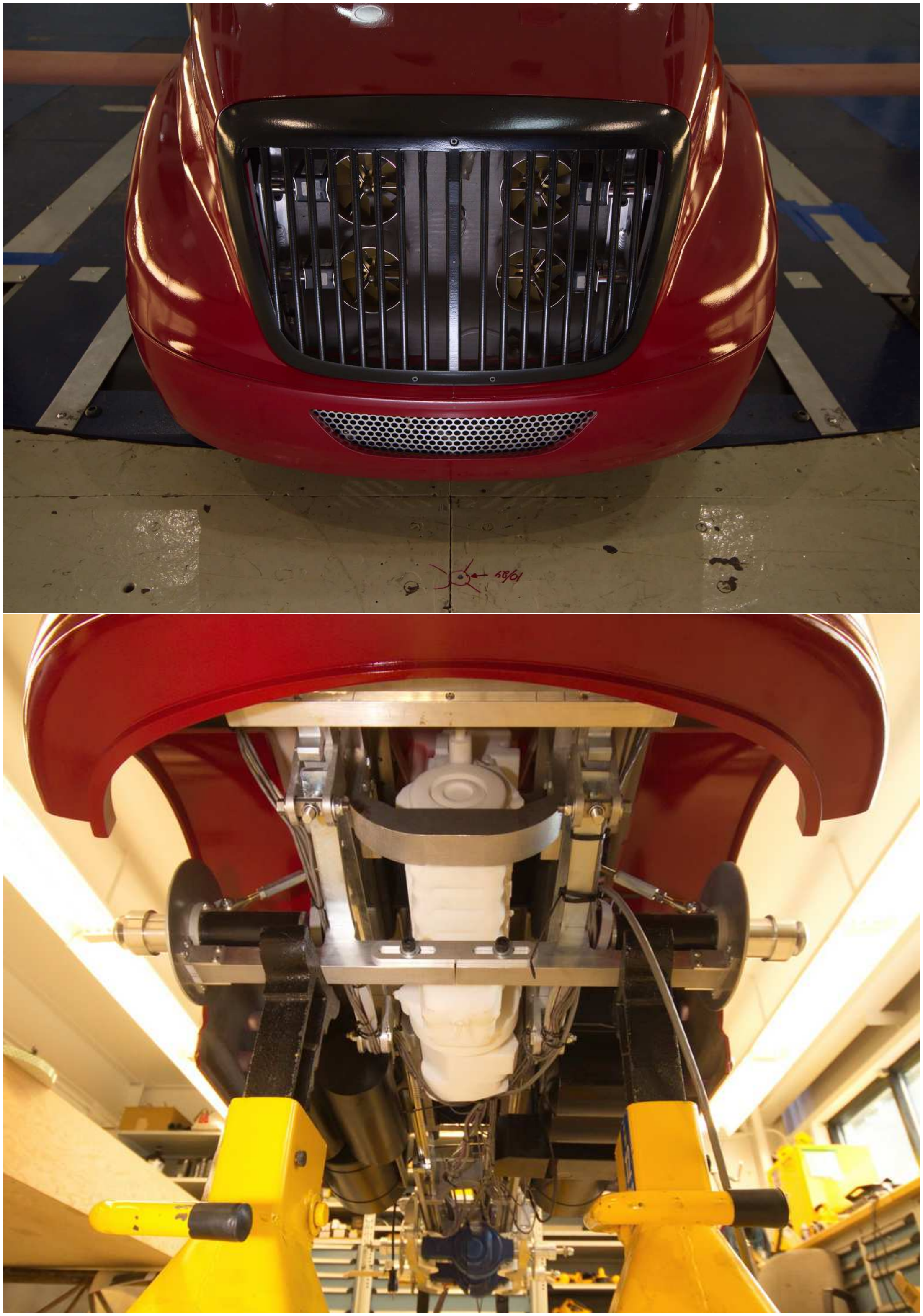

Figure 2.3: Details of the NRC 30%-scale tractor-trailer model including front grille (top), tractor underbody (bottom).

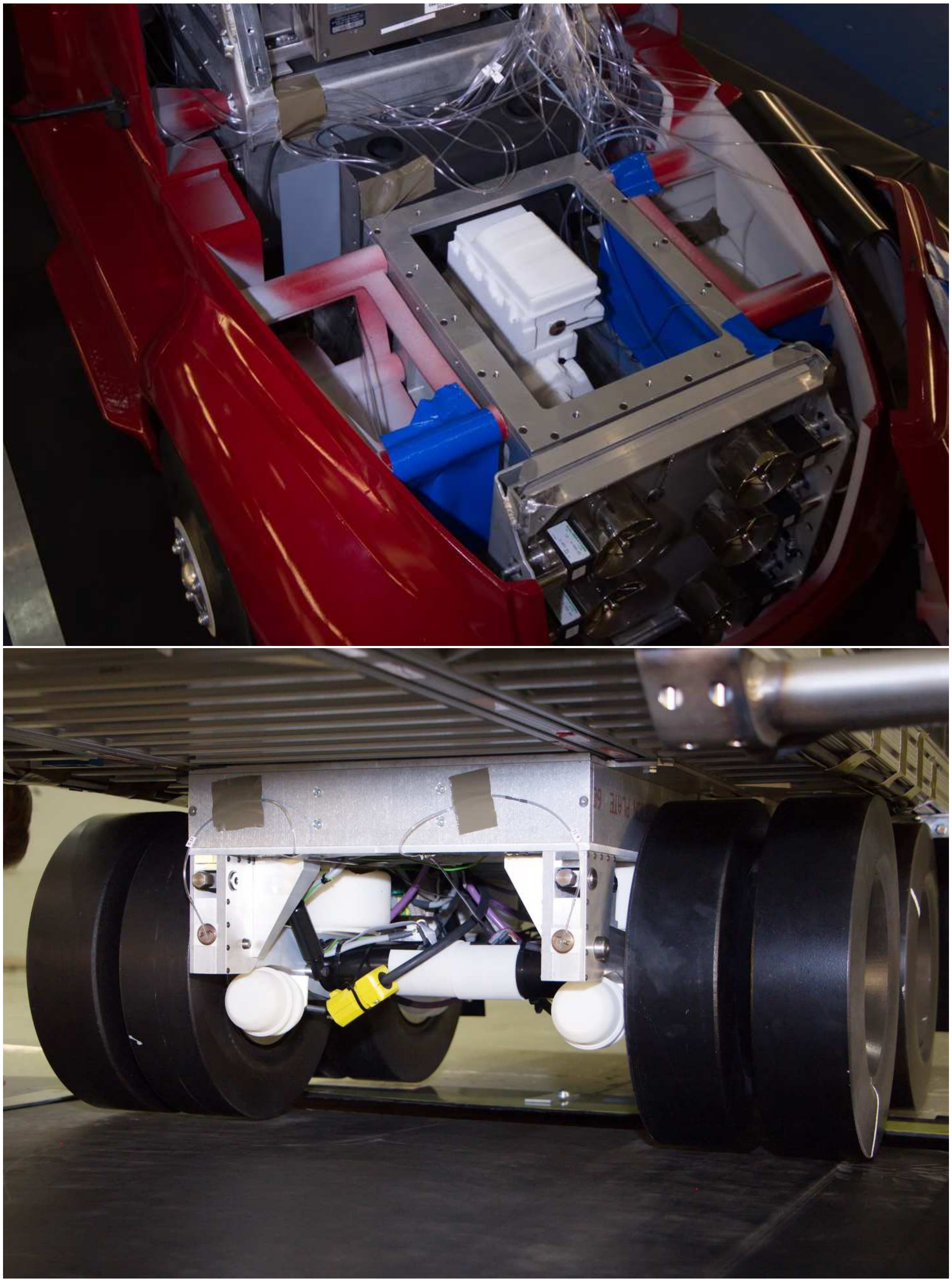

Figure 2.4: Details of the NRC 30%-scale tractor-trailer including engine cavity (top), and trailer wheel assemblies (bottom).

road. The model's wheels are suspended above the belt surface with a maximum clearance of 5 mm. For all but the front cab wheels, the model wheels are above a moving ground plane. The wheels and ground plane are driven at the local airspeed.

Table 2.1: Test-article description.

Tractor Characteristics	
Manufacturer and Model	Adaptation of International ProStar (modified bumper, hood, A-pillar, roof fairing)
Year	characteristic of 2009-present model years
Wheelbase	5.32 m (full-scale)
Tire size	295/75R22.5 on all three axles
Number of axles	3 (6x4 configuration)
Suspension type	leaf-spring on steer axle, air-ride on drive axles
Sleeper type size	56" Hi-Rise Sleeper
Roof fairing type	full-height aerodynamic fairing
Fuel tank sizes	approx. 90 gal
Fuel tank position	mounted to frame rails, covered by tractor side-skirts
Tractor-to-trailer gap	45 inch (full-scale) back of cab to front of trailer (28 inch aero gap, accounting for 17 inch side extenders)
Mud flap location	located behind aft drive wheels
Mud flap type	flexible non-porous (represents rubber mud-flaps)

Trailer Characteristics	
Trailer manufacturer	Features form Wabash and Manac trailers
Trailer type	Dry-van
Trailer axle configuration	tandem
Trailer model year	representative of 2010+ models
Trailer model name	N/A
Trailer length	636 inch, 16.15 m (4.854 m model scale)
Trailer height	Box is 118 inch, 2.99 m (0.899 m model scale) Total is 162 inch, 4.11 m (1.234 m model scale)
Trailer width	102 inch, 2.6 m (0.78 m model scale)
Bogey position	rear of trailer to center of rear axle 120 inch, 3.05 m (0.914 m model scale)
Front corner radius	6 inch, 0.152 m (0.046 m model scale)
Tire size	295/75R22.5 on all axles
Mud flap location	trailer-underside mounted, located behind aft bogie axle
Mud flap type	flexible non-porous (represents rubber mud-flaps)

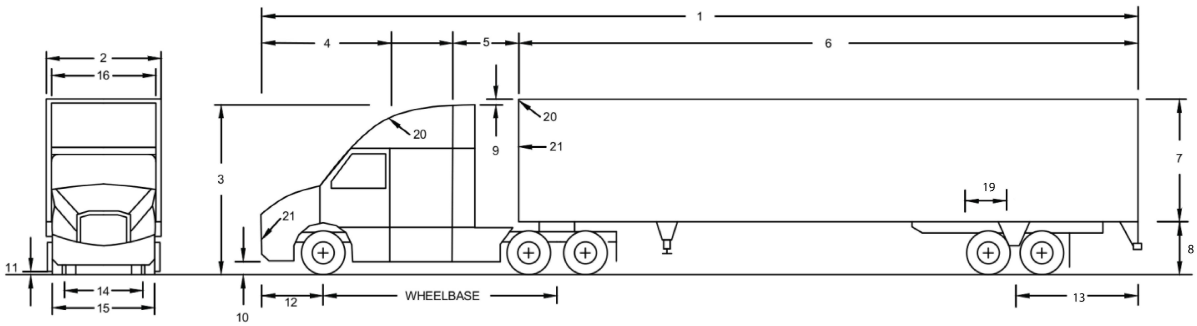

Figure 2.5: NRC 30%-scale tractor-trailer model - locations of relevant dimensions (SAE J1252). Dimensions are listed in Table 2.6.

Figure 2.6: Dimensions of the 30%-scale tractor trailer. Dimensions are indicated in Figure 2.5. Note that dimensions 17 and 18 are not listed in the table as they are indicated as obsolete in SAE J1252.

Characteristic	Dimension in Full Scale
1. Overall length	6.464 m (21.55 m full-scale)
2. Overall Width	0.78 m (2.6 m full-scale)
3. Overall Front Height	1.212 m (4.04 m full-scale)
4. Cab/Sleeper Length	1.275 m (4.25 m full-scale)
5. Gap Length	0.343 m (1.14 m full-scale)
6. Trailer/Box Length	4.854 m (16.15 m)
7. Rear Body Height	0.899 m (2.99 m full-scale)
8. Rear Ground Clearance	0.335 m (1.12 m full-scale)
9. Roof Height Differential	0.022 m (0.075 m full-scale)
10. Front Ground Clearance	0.078 m (0.26 m full-scale)
11. Minimum Ground Clearance	0.078 m (0.26 m full-scale)
12. Front Overhang	0.381 m (1.27 m full-scale)
13. Rear Overhang	1.097 m (3.66 m full-scale)
14. Front Track Width	0.711 m (2.37 m full-scale)
15. Front Bumper Width	0.711 m (2.37 m full-scale)
16. Roof Width	0.719 m (2.40 m full-scale), measured just below chamfer
19. Wheel Diameter	0.305 m (1.02 m full-scale)
20. Leading Edge Geometry	Tractor - Curved, Trailer - Square Edge
21. Front Side Edge Geometry	Tractor - Curved, Trailer - 0.046 m radius (0.15 m full-scale)
22. Wheelbase	1.595 m (5.32 m full-scale)
23. Frontal Area (reference area)	0.959 m2 (10.7 m2 full-scale)

2.2 NRC Trailer Skirts

The NRC Trailer Skirts were developed by NRC for a government research initiative, and designed for the 30%-scale wind tunnel model. The NRC Trailer Skirts consist of a flat-surface design, flush with the sides of the trailer, with a taper at the front edge and mounted to the underbody with L brackets. Photographs and drawings of the NRC Trailer Skirts are included in Appendix A. The wind-tunnel models of the skirts are made of aluminum with sufficient thickness such that they may be considered rigid. These models fasten to the trailer model in a similar manner to how it could fasten to a full-scale trailer.

3. Test Facility

3.1 Background

In the early 1960s, it was found that subsonic wind tunnels in Canada were unable to accommodate vertical or short take-off and landing (V/STOL) aircraft models. V/STOL aircraft research required wind tunnel walls to be further away from the model than the walls of existing conventional wind tunnels. In 1963, following proposals from the aircraft industry, the National Aeronautical Research Committee recommended the construction of what is now the NRC 9 m (30 ft) Wind Tunnel. By 1969, the facility was undergoing the final stages of construction and calibration. Since its commissioning, the NRC 9 m Wind Tunnel has been used for the study of various types of aerodynamic testing, spanning the fields of aeronautics, wind energy, wind engineering, and surface vehicle aerodynamics. The NRC Aerodynamics Laboratory is a member of the Subsonic Aerodynamic Testing Association (SATA) in good standing.

3.2 General Wind Tunnel Characteristics

The NRC 9 m Wind Tunnel is a horizontal closed circuit atmospheric facility with a large test section that is suitable for testing tractor-trailer combinations up to full scale. The test section is preceded by a 6:1 contraction which transitions from a circular cross section to a filleted square cross section. The wind tunnel shell is constructed primarily of welded structural and plate steel. The circuit has a total length of 274 m, an internal duct area of 8,200 m^2, and a total volume of 47,000 m^3. The wind tunnel's fan is powered by an air-cooled 6.7 MW DC motor that provides a maximum wind speed of approximately 55 m/s (200 km/h), or equivalently a dynamic pressure of 1850 Pa, in an empty test section. An external mechanical, pyramidal balance measures the six components of aerodynamic forces and moments. A schematic of the wind tunnel layout is provided Figure 3.1.

The test section of the wind tunnel is surrounded by laboratory and office space, while the remainder of the circuit consists of a steel structure exposed to the outdoors. Downstream of the test section, air flows over breathers which maintain the local atmospheric pressure. Following the breathers, the flow continues through a low-angle diffuser towards a debris screen followed immediately by the first of four 90° bends in the circuit. Over the length of the low-angle diffuser, the cross section the wind tunnel transitions from octagonal (chamfered square) to round. The flow is guided through the bend with the aid of curved steel-plate turning vanes. Turning vanes are present at all corners of the wind tunnel. At the location of the second bend in the wind tunnel, the fan's shaft enters the wind tunnel's shell, shrouded in a streamlined fairing. Following the second bend, the shaft enters the nose cone of the fan assembly. Following the fan, seven anti-swirl vanes straighten the flow. Downstream of the fan section, the air passes once again through a low-angle diffuser towards the third and fourth bends. After the fourth 90° bend, the air enters a wide-angle diffuser complete with wire

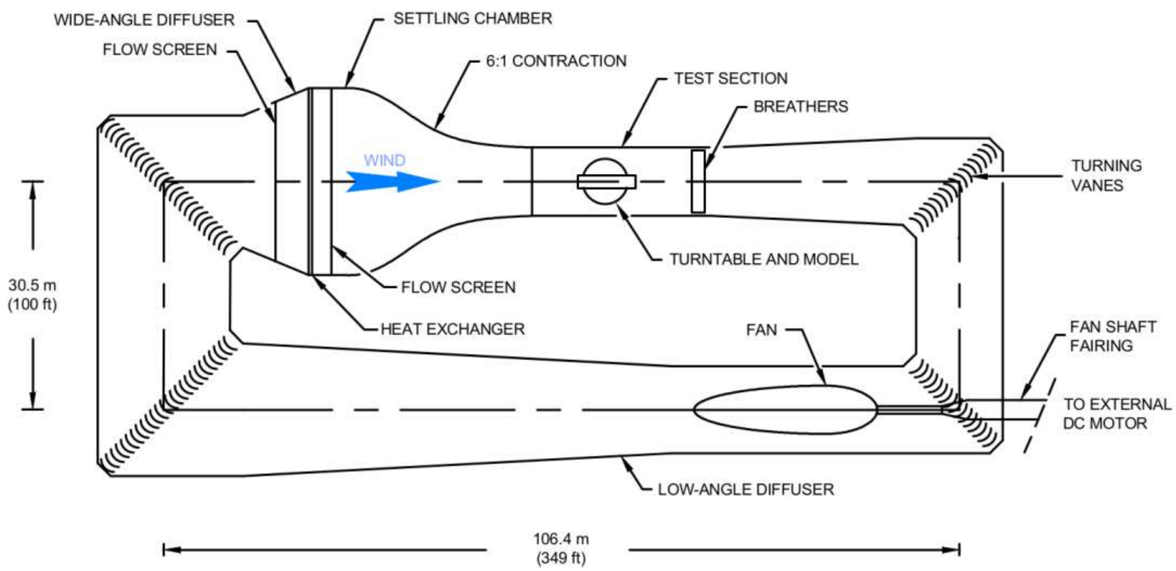

Figure 3.1: Schematic of the NRC 9 m Wind Tunnel.

screen for maintaining flow attachment to the wall. The wide-angle diffuser transitions into a settling chamber which houses a heat exchanger and a screen. The heat exchanger is used exclusively during warm weather to prevent the wind tunnel air and mechanical components from overheating. Following a screen which serves to increase velocity profile uniformity, the air passes through the Road Turbulence System (RTS, described below) and a 6:1 contraction to the test section.

3.3 Test Section Geometry

A drawing of the test section is provided in Figure 3.2. The cross-sectional area of the test section is 82 m^2. From the outlet of the contraction, the walls of the test section diverge slightly (0.1 m over the 23 m length) to accommodate boundary layer growth along the walls and ceiling and prevent the development of a longitudinal static pressure gradient along the test section length. Small openings in the turn table surface allow the model's struts to pass through to connect with a six-axis mechanical pyramidal balance.

3.4 Ground Effect Simulation System

The 30%-scale truck model, which has spinning wheels, was designed for use with the Ground Effect Simulation System (GESS) of the NRC 9 m Wind Tunnel that includes a boundary layer control system (BLCS) and moving ground plane to simulate the appropriate relative motions between the vehicle, the ground, and the air. The BLCS employs two suction plenae to reduce the thickness of the floor boundary layer at the model. The displacement thickness of the

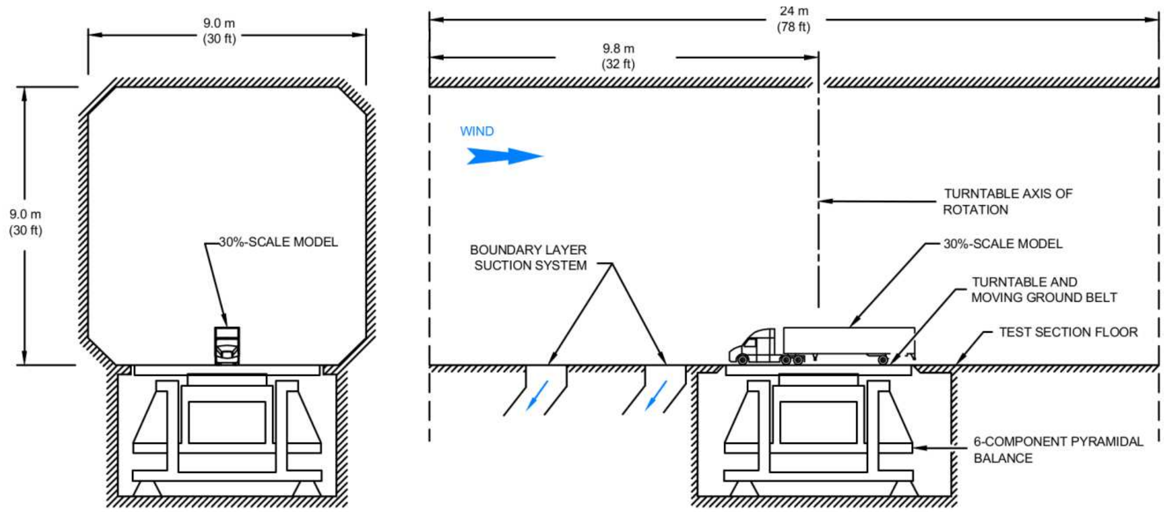

Figure 3.2: Schematic of the test section seen along the direction of wind flow (left) and from the side (right).

boundary layer is 4 mm at the upwind edge of the turntable (same with or without the RTS). At the model, the flow passes over either the smooth surface of 6.1 m diameter turntable, or, over the moving ground plane under and around the model (as in Figures 2.1 and 2.2). The moving ground plane, which consists of a rolling belt system, is contained within the floor turntable and therefore is always moving in the "direction of motion" of the truck. To avoid mechanical fouling between the wheels and the ground plane, the wheels are raised 5 mm from the surface.

The moving ground plane is 5.6 m long, yet the truck model in its SmartWay configuration is 6.5 m long, requiring either the forward part of the model of the back part of the model to overhand the edges of the rolling road and be suspended over the stationary floor. Model commissioning efforts used a 40 ft equivalent trailer (5.2 m length) to examine the influence of the front, the back, or none of the model being suspended over a stationary floor, for which overhanging the front provided no change in drag coefficient, and overhanging the back showed a 3% increase in drag (documented in Appendix D). For trailer-based aerodynamic technologies, the model is configured as in Figure 2.1, with the front of the model suspended over a stationary floor.

3.5 NRC Road Turbulence System

The NRC Road Turbulence System (RTS) is a passive turbulence generating concept using large obstacles mounted in the settling chamber of the NRC 9 m Wind Tunnel. The obstacles are removable, and installed when turbulent flow is desired. The RTS creates a model-scale terrestrial wind environment which replicates what an HDV experiences on typical North-American highways. The system provides a turbulence intensity of 4% with turbulence length-scales greater than 1 m, relative to full-scale conditions. Details of the flow conditions generated by the RTS are provided in Appendix B.

Data collected during the commissioning of 30% tractor-trailer model and RTS indicate that the influence of turbulence from the RTS can be as significant as to cause a 2% reduction in wind averaged drag for the same baseline configuration, and as significant as to cause a 0.5% difference in the drag reduction (relative to the total vehicle wind-averaged drag) with the addition of a device (McAuliffe and D'Auteuil, 2016). For generic trailer-skirt and boat-tail shapes, the drag reductions were shown to be lower in the representative turbulent winds than in the smooth-flow winds typical of many aeronautical and automotive wind tunnels.

The RTS has become part of NRC's best practice for scale-model wind tunnel testing of heavy-duty vehicles. Test results of the NRC Trailer Skirts are presented based on measurements using the RTS in the NRC 9 m Wind Tunnel.

3.6 Test Section Flow Characteristics

The maximum wind speed possible with an empty test section is 55 m/s. This corresponds to a dynamic pressure of approximately 1850 Pa. For the purpose of SmartWay testing with the 30%-scale tractor trailer combination, the wind tunnel's wind speed is set to 50 m/s, based on limitations of the moving ground plane. This corresponds to a Mach number of 0.12 and a model-width based Reynolds number of approximately 2.6 million. The Reynolds number is above one million, as required by SmartWay protocols. The Mach number is below 0.25, therefore considerations due to compressibility are unnecessary (*SAE Wind Tunnel Test Procedure for Trucks and Busses*, 2012).

In the vicinity of the model, without influence of the RTS, the static pressure gradient is below 0.001 m^{-1} (Clark, 2010), and the turbulence intensity is approximately 0.5%. Under these condition, the boundary layer at the leading edge of the turn table has a displacement thickness of 4 mm and an angularity less than 0.06° (Larose *et al.*, 2001). With the RTS installed, the displacement thickness is also 4 mm.

For closed-test sections, NRC's best practice is to maximize the distance between the aft end of the model and the test-section diffuser, such that the model is upstream of the diffuser by at least 4 times the average width of the model, to eliminate the potential for pressure field changes at the end of the test section to adversely affect the wake and the vehicle drag. The distance between the aft end of the 30%-scale trailer and the diffuser is approximately 11 m, which is greater than 10 model-widths, and therefore no adverse diffuser-proximity effects influence the measurement results.

The turbulence generated by the RTS is similar to representative turbulence characteristics experienced by heavy-duty vehicles on Canadian roads, with a turbulence intensity of 4% and a turbulence length scale greater than 1 m, as described in Appendix B.

3.7 Fan Section Details

The wind tunnel is powered by a single propeller fan, located downstream of the second corner (Figure 3.1). The fan section is a 27.4 m long and 11.6 m in diameter. The fan consists of a stationary nose cone, followed by a rotor to which eight fan blades are fastened, followed by a stationary tapered structure supported by seven anti-swirl vanes. The fan is driven via a shaft by a 6.7 MW DC motor, housed outside the wind tunnel in a separate adjacent building. The shaft is enclosed in a fairing designed to minimize power loss in the circuit and the effect of its wake on the fan around the corner. To achieve 50 m/s in the test section, the fan rotates at approximately 214 RPM (tip speed of 130 m/s).

3.8 Wind Tunnel Control and Data Acquisition

The wind tunnel conditions are set by controlling the fan speed, the yaw angle of the model, the speed of the model wheels, the speed of the moving ground plane underneath the model, and the speed of the BLCS motors. Measurements of relevance to SmartWay testing include dynamic pressure, drag force, side force, wheel motor voltage, and wheel motor current.

During testing, the operator is able to set the fan speed and the angle of the turntable. A National Instruments PXI system is used to control the fan speed and turntable position. Typically, the standard deviation of the fan speed is below 0.16 RPM, and the resolution of the model angle is 0.01°. The speed of the model wheels, moving ground plane, and BLCS motors are indirectly controlled by the set conditions of the wind tunnel (fan speed, selected blockage correction), and measured conditions (air temperature, relative humidity, absolute pressure). Automated scripts are used to defined turntable angle maps for the SmartWay-defined yaw-angle conditions.

Dynamic pressure is measured at the exit of the contraction, far away from influences of the model. Measurements are made with an MKS model 698A Baratron heated, high accuracy, differential capacitance manometer. The temperature, relative humidity, and absolute pressure of the air are measured in the settling chamber by eight RTDs, a Rotronic C94 model MP101A hygrometer, and a Paroscientific model 740-16B digital barometer respectively. Wind tunnel calibrations are used to calculate the corresponding dynamic pressure in an empty test section in real time, and standard blockage correction techniques are used to account for the increased dynamic pressure due to the presence of the model. The blockage-corrected dynamic pressure, together with the measured properties of the air, is used to calculate the wind speed in the test section. This wind speed is used to determine the appropriate speed of the moving ground plane, and the speed of the moving ground plane is in turn used to control the rotational speed of the model wheels via the supplied voltage to each motor (Maxon DC motor, RE 50, Graphite Brushes).

Force measurements are obtained from a six-axis pyramidal mechanical balance. In the range used for the present work, the balance has a resolution of 0.4781 N in drag and 1.209 N in side force, measured in wind tunnel coordinate system. The increments of the resolution are referred to as “balance counts.” Tare values are recorded in a closed test section with still air, immediately before testing, over the range of yaw angles to be tested. New tare values are recorded after significant model changes or when the balance does not return to within three balance counts of drag or side force due to thermal effects.

3.9 Quality Management Certification

The NRC Aerospace Portfolio, including the Aerodynamics Laboratory, has ISO 9001 certification. All critical instrumentation is calibrated following appropriate calibration schedules, and all calibrations are documented and traceable. Facility validations and verifications are performed as part of the certified quality management process.

3.10 Previously Published Test Results

To date, two peer-reviewed journal paper have been published by SAE pertaining to testing with the 30%-scale tractor-trailer model in the NRC 9 m Wind Tunnel. McAuliffe and D'Auteuil (2016) documents the development of the RTS and its influence on the drag performance of the 30%-scale truck model. McAuliffe and Wall (2016) documents a study that evaluated various design parameters for boat-tails, as well as the variability of boat-tail performance with changes to the vehicle configuration.

4. Test Method

4.1 Test Procedure

The test consists of seven runs. The first three runs establish the wind-averaged coefficient of drag, WAC_D, of the model without the addition of the aerodynamic device. These runs are referred to as baseline runs, and the average WAC_D from these three runs is referred to as the starting baseline. The fourth, fifth, and sixth runs establish the WAC_D of the model equipped with the aerodynamic device. These runs are referred to as the test runs. In a seventh and final run, the device is removed and the model is returned it to its baseline configuration. The final run is referred to as the follow-up baseline. For each run, time series of measurements are taken with the model at yaw angles of 0°, -9°, -6°, -3°, -1°, 0°, 1°, 3°, 6°, 9°, and 0°relative to the wind-tunnel axis. Measurements are taken over a duration long enough such that the random uncertainties in average values are small compared to the bias uncertainties of the instruments. The WAC_D is subsequently determined from the drag coefficients of the model over a range of wind angles relative to the vehicle. Details of the calculation procedure are described below in Section 4.2.

For the data to be deemed acceptable, the following conditions must be satisfied in seven consecutive runs:

1. For each run, the first and last measurement of the drag coefficient at a zero degree yaw angle are no more than 0.5% apart;
2. The wind averaged drag coefficients of the three baseline runs are no more than 0.5% apart;
3. The wind averaged drag coefficients of the three device runs are no more than 0.5% apart; and
4. The follow-up baseline and the starting baseline are no more than 0.5% apart.

4.2 Data Reduction

The wind tunnel data provides wheel power, wind speed, properties of the air, and aerodynamic force and moment data in the coordinate system of the wind tunnel. From the acquired wind tunnel data, and after conversion from acquired values to appropriate SI units, the process of data reduction consists of:

1. Calculating the reference dynamic pressure and static pressure in the test section based on the wind tunnel calibration;
2. Calculating the flow parameters in the test section (air properties and wind speed) using standard fluid dynamics equations;

3. Calculating the force and moment coefficients at the balance resolution centre;
4. Translating the moment coefficients to the reference location (client specified location);
5. Calculating and applying wall corrections to the flow parameters and to the force and moment coefficients, correcting the force and moment coefficients to account for wind tunnel blockage, and correcting the yaw angle for wall interference;
6. Rotating force and moment coefficients from a test-section coordinate system to a model axis coordinate system;
7. Calculating the aerodynamic torque from all wheel motors, formulating an effective model-axis force coefficient, correcting for blockage, and adding it to the model-axis drag coefficient;
8. Applying strut-tare and interference corrections to the force and moment coefficient, appropriately accounting for the blockage corrections;
9. Performing calculations and corrections for other measurements such as surface pressures and front-grille anemometers;
10. Calculating the potential fuel savings according to the calculations and assumptions of Section 4.2.5.

Additionally, the uncertainty of the wind-averaged drag coefficient and the potential fuel savings is calculated to ensure the verification category of the device may be chosen with a high level (95%) of confidence. The following sections provide an overview of these steps.

4.2.1 Wall Interference Corrections

To account for confinement of the flow within the closed-wall test section, two forms of corrections are applied:

- Blockage Corrections: The Thom-Heriot blockage-correction method (SAE SP-1176, 1996) is applied for heavy-duty vehicle testing in the NRC 9 m Wind Tunnel. The method makes use of model and test-section geometry, and the model force coefficients, to determine a dynamic pressure correction and wake-drag-increment correction that are appropriately applied to the force and moment coefficients.
- Wind Angle Corrections: At yaw, the interaction of the model side force on the flow and the presence of the test section walls influence the flow-field around the model in a manner equivalent to increasing the relative wind/yaw angle. This is corrected using standard wind tunnel methods (Barlow *et al.*, 1999).

4.2.2 Strut Influence Corrections

The six model mounting struts are not shielded from the wind and therefore any wind-loads measurements contain a component associated with the strut, called the strut tare loads. The strut-tare drag loads are on the order of 5% of the model drag, necessitating correction of the measured data. Characterization of the wind loads experienced by the struts (strut tare loads) was performed when the 30%-scale truck model commissioning efforts were undertaken. Measurements of the strut wind loads were performed in a configuration in which the struts were connected to the balance and the model was supported rigidly to the test section floor without contacting the struts. Strut-tare loads were recorded over a large range of model yaw angles (±15°), converted to coefficient form, and fitted with a high-order polynomial to allow ease of application when correcting the model wind-load measurements.

The presence of the struts also influence the wind patterns and the wind loads experienced by the model, but to a lesser extent than the strut tare loads (1-2%). These strut interference loads are estimated based on measurements performed at 1/10 scale with a truck model in the NRC 2 m × 3 m Wind Tunnel as part of the strut design process. Those measurements were fitted with similar high-order polynomials, and are used to correct the drag-coefficient data in a similar manner as the strut-tare corrections.

4.2.3 Aerodynamic Resistance of the Wheels

The overall aerodynamic resistance to the motion of a ground vehicle includes the drag force acting on the vehicle, in-line with the direction of motion, as well as the aerodynamic torque experienced by the wheels. The engine must account for both aerodynamic resistances, and hence, both aerodynamic resistances play a role in fuel consumption. To incorporate aerodynamic torque in the calculation of potential fuel savings (below), wheel torque is converted to an effective drag force acting on the model, converted to coefficient form, and added to the "in-line" drag coefficient, C_D. The resulting drag coefficient, which includes the contribution of wheel resistance, and the effective drag force are

$$C_{D,W} = C_D + \frac{D_W}{Q_C A} \tag{4.1}$$

where

$$D_W = \sum \frac{(I_{WIND} - I_0)\tau}{r} \tag{4.2}$$

and where D_W is the effective drag due to the wheels, calculated as the sum of effective drag contributions from each wheel. I_{WIND} is the current supplied to the motor during testing, I_0 is a no-load current removed as a tare, τ is the torque coefficient of the motor and r is the radius of the wheel.

Once converted to a force coefficient, the effective wheel-torque drag is on the order of 2-4% of the model drag.

4.2.4 Wind-Averaged Coefficient of Drag

The wind-averaged coefficient of drag, WAC_D, is defined as:

$$WAC_D(U_g) = \frac{1}{2\pi} \int_0^{2\pi} C_{D,W}(\eta) \left[1 + \left(\frac{U_{avg}}{U_g} \right)^2 + 2 \left(\frac{U_{avg}}{U_g} \right) \cos\theta \right] d\theta \tag{4.3}$$

where

$$\eta = \tan^{-1} \left[\frac{(U_{avg}/U_g) \sin\theta}{1 + (U_{avg}/U_g) \cos\theta} \right] \tag{4.4}$$

in which U_g is the vehicle ground speed, η is the vehicle-referenced wind angle, U_{avg} is the mean terrestrial wind speed, and θ is the terrestrial wind angle. For Canada and the United States, a typical mean terrestrial wind speed (U_g) used for these calculations is 11 km/h or 7 mph (*SAE Wind Tunnel Test Procedure for Trucks and Busses*, 2012). Note that the calculation of WAC_D uses the effective drag coefficient $C_{D,W}$, which includes the aerodynamic resistance to wheel rotation. Following the test, WAC_D is evaluated for ground speeds of 80.5 km/h, 88.5 km/h, 96.6 km/h, 104.6 km/h, 112.7 km/h, and 120.7 km/h (50 mph, 55 mph, 60 mph, 65 mph, 70 mph, and 75 mph respectively). WAC_D will be evaluated using the approximation of the above integral outlined in Section A.2 of *SAE Wind Tunnel Test Procedure for Trucks and Busses* (2012).

4.2.5 Calculation of Potential Fuel Savings

Several methods exist for estimating fuel savings from aerodynamic measurements. Per the EPA SmartWay procedures, the change in fuel consumption associated with changes in aerodynamic drag are estimated based on fuel economy estimates developed by McCallen *et al.* (1999). Table 4.1 lists the conversion factors used to convert the wind-tunnel measurements to fuel savings based on this method.

Table 4.1: Conversion factors to estimate fuel savings from wind-averaged-drag reduction measurements.

Ground Speed (mph)	Conversion factor $CF = \Delta WAC_D/\Delta f$
50	2.30
55	2.15
60	2.00
65	1.85
70	1.75
75	1.50

The estimated fuel savings is calculated as:

$$\Delta f[\%] = \frac{1}{CF} \times \frac{\Delta WAC_D}{WAC_D} \times 100 \tag{4.5}$$

where CF is the conversion factor from Table 4.1 associated with the equivalent ground speed from which the wind-averaged-drag coefficients were evaluated. SmartWay procedures use 65 mph as the reference ground speed at which to evaluate the fuel savings (CF = 1.85) and therefore the fuel savings is calculated as

$$\Delta f[\%] = 54.1 \times \frac{\Delta WAC_D}{WAC_D} \tag{4.6}$$

The value of Δf is used to determine into which category, if any, the tested aerodynamic device will be verified by the EPA.

4.2.6 Uncertainty Requirements and Calculation

The calculated improvement to fuel consumption is associated with an uncertainty, $\delta\Delta f$, such that the true value potential fuel savings is in the interval $\Delta f \pm \delta\Delta f$.

The magnitude of $\delta\Delta f$ depends on how Δf is calculated and the elemental uncertainties in measured quantities used to calculate Δf. For the purpose of selecting a verification category, it should be shown that the interval defined by $\Delta f \pm \delta\Delta f$ is above the lower threshold of the category. To be verified in the "1%" category, the lowest verification category offered by the EPA, Δf must be greater than 1% + $\delta\Delta f$.

The magnitude of $\delta\Delta f$ is evaluated analytically by following a standard uncertainty analysis procedures (Coleman and Steele, 1995). The analysis considers random uncertainties arising from fluctuating measurands and elemental random and bias uncertainties associated with the instrumentation and calibrations. Elemental uncertainties have been determined from instrument specifications and statistical analysis of the wind tunnel calibration (the relationship between measured dynamic pressure and dynamic pressure in an empty test section). A coverage factor of 2 is used to calculate an expanded uncertainty interval reflecting a level of confidence of 95% (Taylor and Kuyatt, 1994). The uncertainty analysis includes correlated bias uncertainties through the Sum of Products Approximation method, proposed and validated through a Monte Carlo simulation, by Brown *et al.* (1996).

5. Wind Tunnel Test Results

The NRC Trailer Skirts were evaluated in November 2014 in the NRC 9 m Wind Tunnel with the NRC 30%-scale tractor trailer model, the results of which are shown in Figure 5.1. The variation of drag coefficient (C_D) with yaw angle for the reference vehicle configuration and the NRC Trailer Skirts configuration are shown in the left-hand graph of Figure 5.1, with the changes in wind-averaged drag coefficient (ΔWAC_D, evaluated at 65 mph ground speed) are shown in the right-hand graph. In addition, the variations in drag-coefficient reduction (ΔC_D), are also plotted in the left-hand graph of Figure 5.1 to provide a measure of how the devices perform with changes of wind direction. The results of Figure 5.1 show good repeatability in the measurements, for both the baseline vehicle and that equipped with the NRC Trailer Skirts. The NRC Trailer Skirts provide a reduction in wind-averaged-drag coefficient of 0.0572, or 9.9%. The data presented in Figure 5.1 is tabulated in Appendix C.

Table 5.1 provides the drag-coefficient reductions and the fuel-savings estimates for the NRC Trailer Skirts, which shows a fuel savings of 5.4%. With four reference runs and three device runs, the uncertainty evaluated for the fuel savings is ±0.1%. If only the first device run is used for the calculations, instead of all three, the numbers in Table 5.1 remain the same. The uncertainty on the fuel savings is actually 0.05% for the three-device-run calculation and 0.11% for the single-device-run calculation, and therefore both round to 0.1%. These uncertainty values assume that the conversion factor of 1.85 between wind-averaged-drag coefficient and fuel savings has no quantifiable uncertainty, which is a reasonable assumption for the purpose of this report given that EPA SmartWay will use these results to compare to other technology results reported in the same manner using the same conversion factor.

Table 5.1: Performance results and fuel-savings estimate for the NRC Trailer Skirts.

Configuration	Wind-averaged drag coefficient WAC_D	Change in wind-averaged drag coefficient ΔWAC_D	Fuel savings estimate Δf
Reference	0.5760	-	-
NRC Trailer Skirts	0.5188	-0.0572 (-9.9%)	5.4 ± 0.1 %

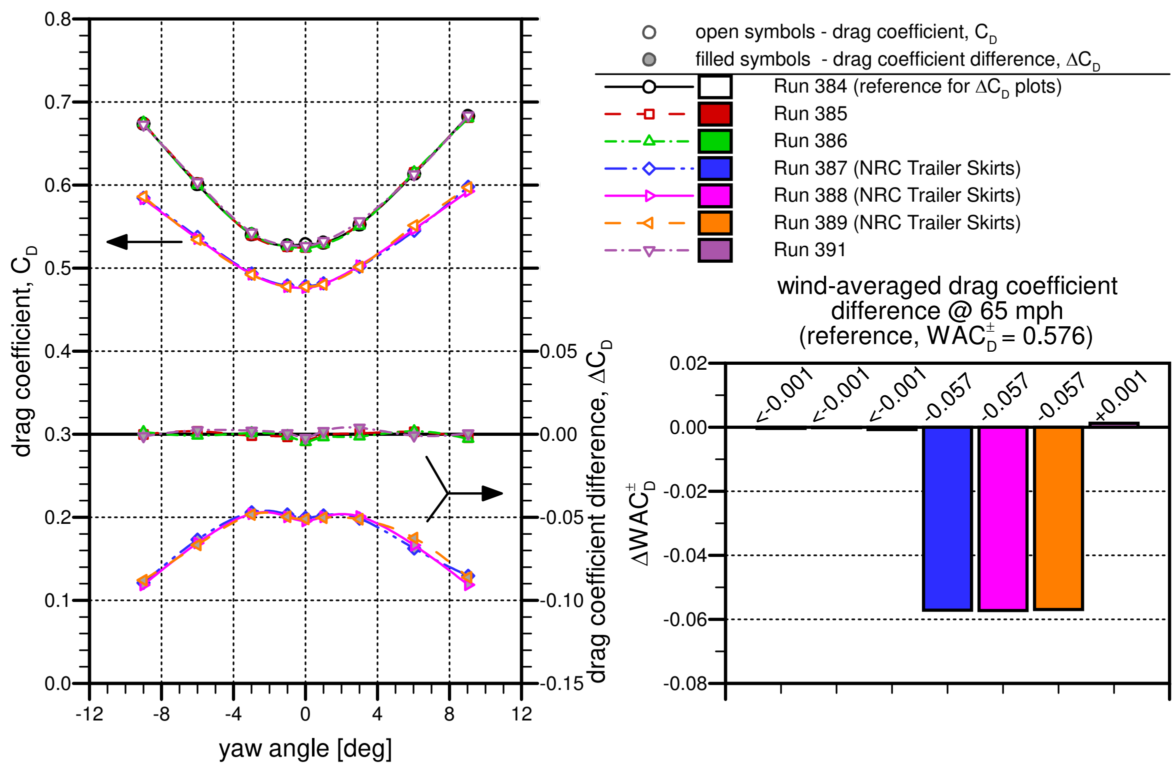

Figure 5.1: Wind tunnel test results for NRC Trailer Skirts.

6. Summary and Conclusions

The *NRC Trailer Skirts* design has been tested in the NRC 9 m Wind Tunnel according to EPA SmartWay verification protocols. The device was tested on a 30%-scale model of a tractor-trailer combination configured appropriately for SmartWay verification tests. Testing consisted of three starting baseline runs, three test runs with the *NRC Trailer Skirts* mounted to the model, and a follow-up baseline run. For each run, the drag coefficient was measured over a range of yaw angles with sufficient resolution to calculate a wind-averaged drag coefficient. The *NRC Trailer Skirts* were measured to have a reduction in wind averaged drag of 9.9% which is estimated to provide a fuel savings of 5.4±0.1%. Using a single test run instead of three provides identical fuel-savings results and uncertainty levels, within the precision of the reported results.

References

Barlow, J. B., Rae, W. H. and Pope, A. (1999), *Low-Speed Wind Tunnel Testing*, 3^{rd} ed., Wiley-Interscience.

Brown, K. K., Coleman, H. W., Steele, W. G. and Taylor, R. P. (1996), "Evaluation of Correlated Bias Approximations in Experimental Uncertainty Analysis," AIAA Journal, **34**, pp. 1013–1018.

Clark, C. (2010), "A Study of the flow conditions for ground-vehicle testing in the 9 m x 9 m wind tunnel facility with the GESS installed," NRC Report No. LTR-AL-2010-0022, *National Research Council Canada*.

Coleman, H. and Steele, W. G. (1995), "Engineering Application of Experimental Uncertainty Analysis," AIAA Journal, **33**, pp. 1888–1896.

EPA (2015), "EPA SmartWay Verification Test Procedure for Determining Fuel Savings: Scale Wind Tunnels," Version 1 , *U.S. Environmental Protection Agency*.

Kirchhefer, A. J. and McAuliffe, B. R. (2015), "NRC Trailer Skirts - SmartWay Testing Using the NRC 9 m Wind Tunnel - Pre-Test Report," NRC Report No. LTR-AL-2015-0053, *National Research Council Canada*.

Larose, G., Tanguay, B., Van Every, D. and Bender, T. (2001), "The New Boundary Layer Control System for NRC's 9 m x 9 m Wind Tunnel," *AIAA* 39^{th} *Aerospace Sciences Meeting & Exhibit*, Reno, Nevada.

McAuliffe, B. R., Belluz, L. and Belzile, M. (2014a), "Measurement of the On-Road Turbulence Environment Experienced by Heavy Duty Vehicles," SAE Int. J. Commer. Veh., **7(2),** doi: 10.4271/2014-01-2451.

McAuliffe, B. R. and D'Auteuil, A. (2016), "A System for Simulating Road-Representative Atmospheric Turbulence for Ground Vehicles in a Large Wind Tunnel," SAE Int. J. Passeng. Cars - Mech. Syst., **9(2),** doi: 10.4271/2014-01-2451.

McAuliffe, B. R. and Wall, A. S. (2016), "Aerodynamic Performance of Flat-Panel Boat-Tails and Their Interactive Benefits with Side-Skirts," SAE Int. J. Commer. Veh., **9(2),** doi: 10.4271/2016-01-8015.

McCallen, R., Couch, R., Hsu, J., Leaonard, A., Brady, M., a. R. J., Storms, B., Heineck, J. T., Driver, D., Bell, J., Zilliac, G., Browand, F., Hammache, M., Salari, K. and Rutledge, W. (1999), "Progress in Reducing Aerodynamic Drag for Higher Efficiency of Heavy Duty Trucks (Class 7-8)," SAE Paper No. 1999-01-2238.

SAE SP-1176 (1996), "Closed-Test-Section Wind Tunnel Blockage Corrections for Road Vehicles," SAE Special Publication No. SP-1176, *SAE International*.

SAE Wind Tunnel Test Procedure for Trucks and Busses (2012), "SAE Wind Tunnel Test Procedure for Trucks and Busses," 2012.

Taylor, B. N. and Kuyatt, C. E. (1994), "Guidelines for Evaluating and Expressing the Uncertainty of NIST Measurement Results," NIST Technical Note No. 1297, *United States Department of Commerce Technology Administration - National Institute of Standards and Technology*.

A. NRC Trailer Skirts - Photographs and Drawings

The NRC Trailer Skirts were designed as a simple flat panel to be mounted flush to the side of the trailer. Photograph of the 30%-scale truck model with and without the NRC Trailer Skirts are shown in Figures A.1 and A.2. The wind-tunnel models of the NRC Trailer Skirts were fabricated using 3/8 inch thick aluminum panels, with L-shaped under-trailer mounting brackets, as shown in Figure A.3. The dimensions of the NRC Trailer Skirts are provided in Figure A.4.

Figure A.1: Photograph of NRC 30%-scale tractor-trailer model with NRC Trailer Skirts - front view.

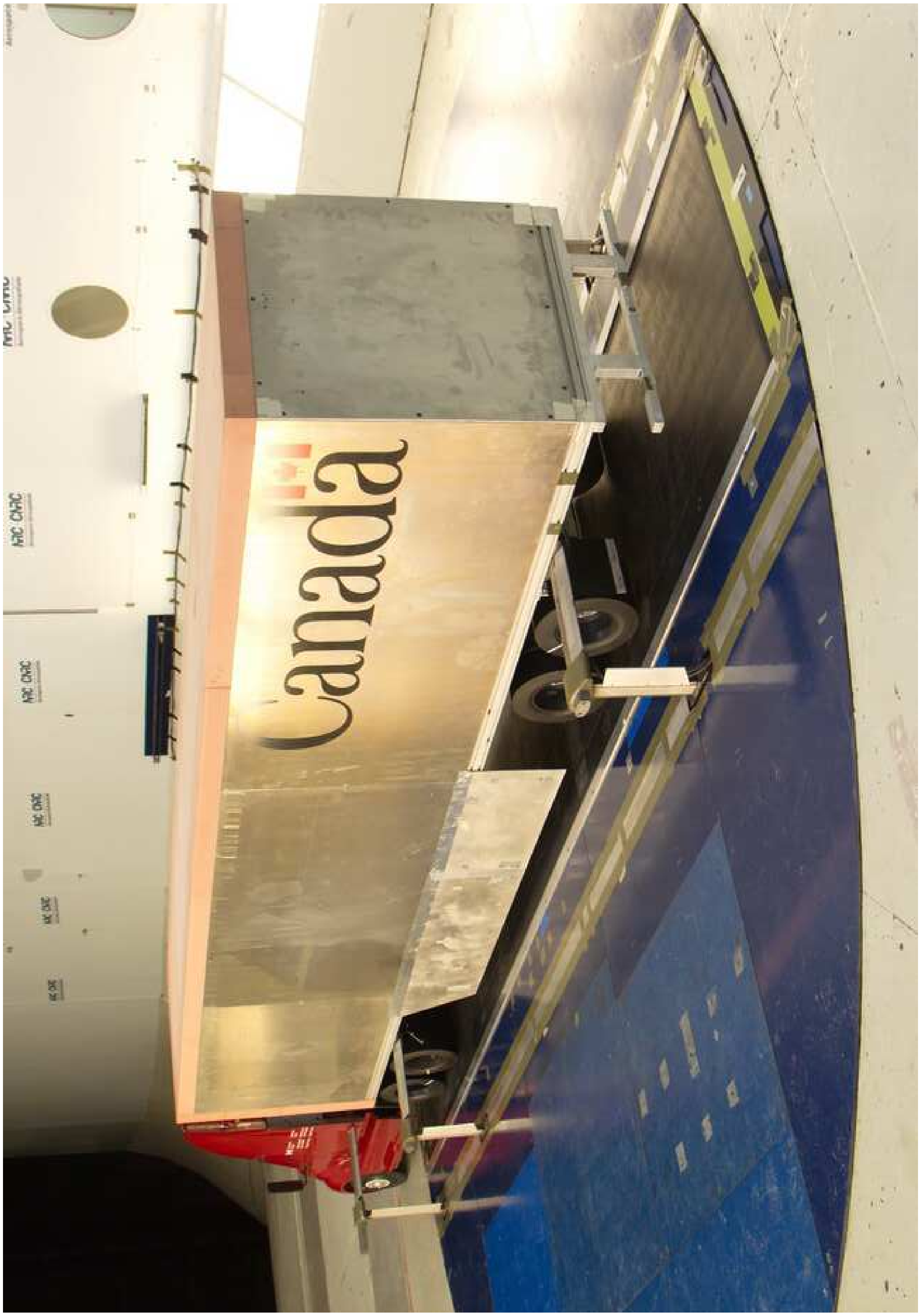

Figure A.2: Photographs of NRC 30%-scale tractor-trailer model with NRC Trailer Skirts - rear view.

Figure A.3: The wind tunnel model of the NRC Trailer Skirts. The skirts are shown installed on the bottom of the overturned model trailer (top) with a close-up view of the mounting brackets (bottom).

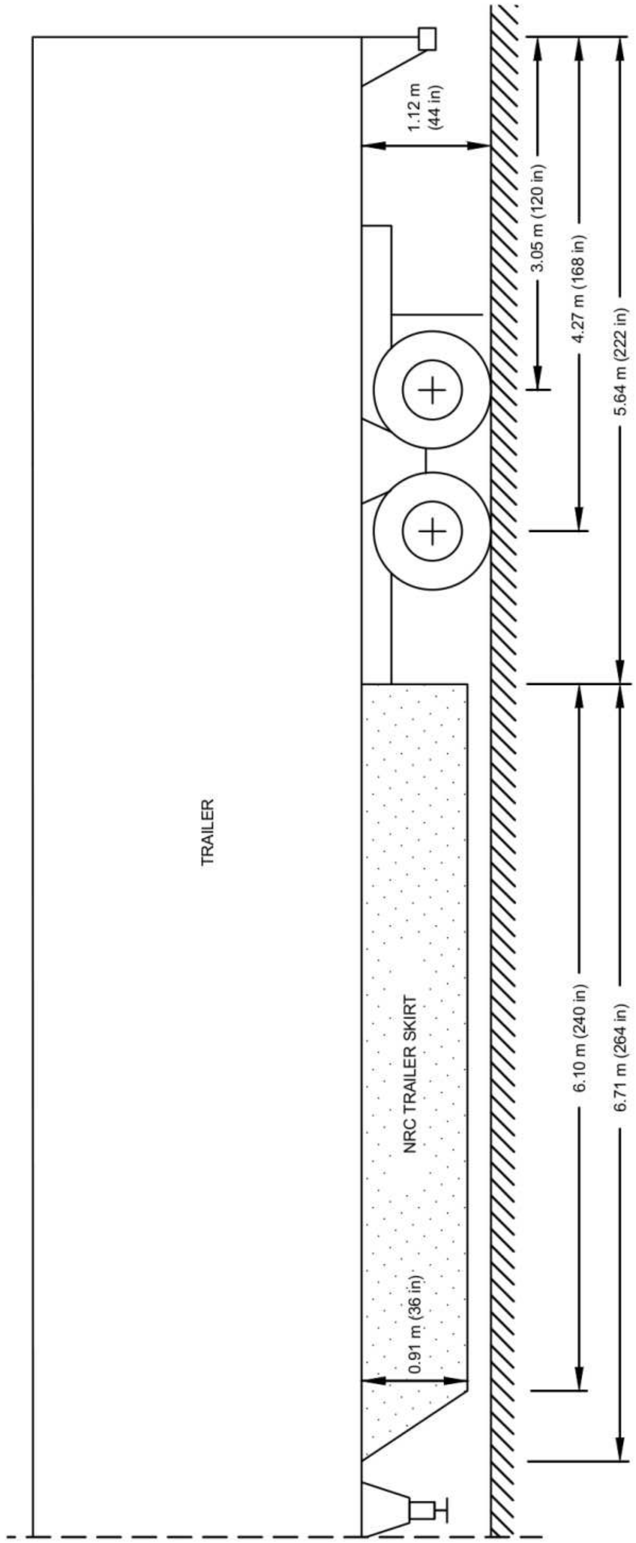

Figure A.4: Dimensions and placement of the NRC Truck Skirts on a tractor trailer. Full scale dimensions are indicated.

B. Flow Specifications for the NRC Road Turbulence System (RTS)

The NRC Road Turbulence System (RTS) is a passive turbulence generation system for the NRC 9m Wind Tunnel that has been designed to simulate typical turbulence characteristics encountered by ground vehicles in highway driving conditions. The system was developed to match wind spectra measured on the road, based on the road measurements of McAuliffe *et al.* (2014a). These road measurements results identified a target condition, and identified that the turbulence conditions encountered on the road are most sensitive to traffic density, associated with the wakes of other vehicles on the road. Table B.1 provides the turbulence intensity and length scales measured 0.45 m from the floor of the 9m Wind Tunnel (equivalent to 1.5 m full scale above ground for the 30%-scale model), and compares them to the target road measurements. Figure B.1 shows the measured wind spectra from the RTS, compared with that measured on the road for four levels of traffic density, and Figure B.2 shows the horizontal spatial correlation of the turbulence compared to road measurements for three levels of traffic density. The range of traffic density varied between light (very few vehicles if any) through dense (many vehicles in close proximity while maintaining a road speed of 100 km/h), and includes traveling in the wake of a heavy-duty vehicle (HDV wake).

The tabulated RTS data in Table B.1 show similar trends in comparison to the road measurements, with similar magnitudes of the various component intensities and length scales compared to their road-measured values. The wind spectra measurements of Figure B.1 are presented based on the reduced frequency which allows a direct comparison of road and wind tunnel measurements at different scales. The reduced frequency is defined in such a way that its reciprocal represents a wavelength in meters at full scale. The wind spectra for all three velocity components match well the target moderate traffic conditions for reduced frequencies greater than 0.1 (wavelengths smaller than 10 m). At lower reduced frequencies the longitudinal component (in-line with the direction of motions of the vehicle) contains less turbulence energy, and the lateral and vertical components contain more energy. Despite these differ-

Table B.1: Measured turbulence characteristics of the RTS for the 30%-scale tractor-trailer model compared to target road measurements (length scales represent full-scale equivalent values conditions, and measurements made at an equivalent 1.5 m height from ground.

Component	**Turbulence Intensity, I**		**Turbulence Length Scale, L^x**	
	Road	**RTS**	**Road**	**RTS†**
u	4.0 %	3.8 %	4.7 m	1.1 m
v	3.5 %	5.0 %	1.9 m	2.4 m
w	3.1 %	4.9 %	0.6 m	1.7 m

† full-scale equivalent

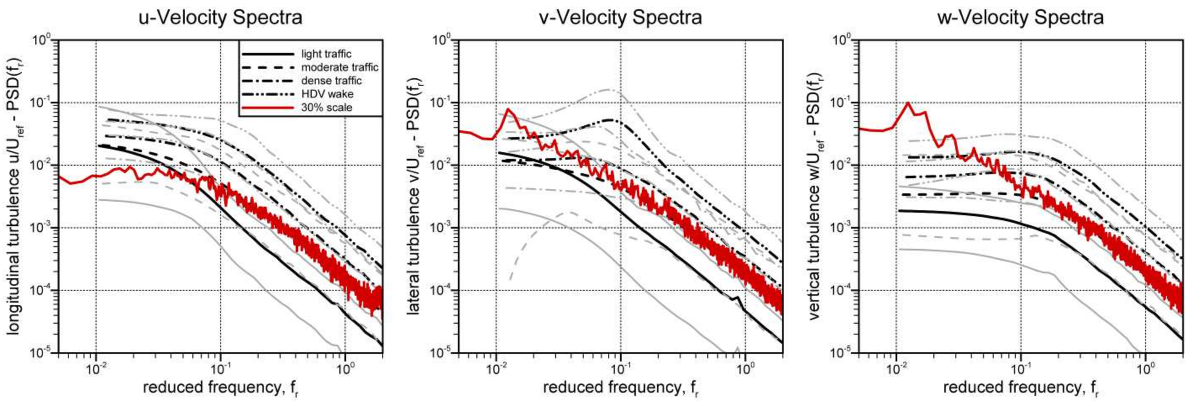

Figure B.1: Spectra of the longitudinal, lateral and vertical wind components measured for the RTS in the NRC 9 m Wind Tunnel compared with the on-road measurements (measurements made at an equivalent 1.5 m from ground level).

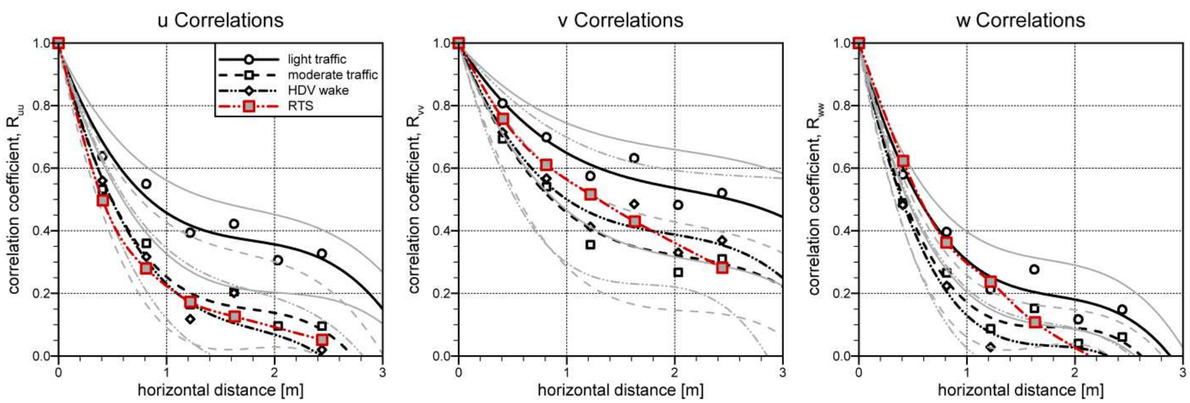

Figure B.2: Horizontal spatial correlation measurements for the RTS compared to on-road measurements for different traffic densities (measurements made at an equivalent 1.5 m from ground level).

ences, the turbulence energy is mostly within the range maximum and minimum range of on-road measurements as defined by the grey lines in the plots. The spatial correlation measurements of Figure B.2 show that the spatial scales of turbulence of the RTS are also well matched to the target moderate traffic road measurements.

Uniformity of the mean flow speed is approximately $\pm 1\%$ over the vertical and horizontal extent of the 30%-scale truck model (region 1.5 m high and 3 m wide, equivalent to 5 m and 10 m full scale). Flow angularity is within ± 1 over this same range. With the boundary layer suction system active, the displacement thickness at the front edge of the turntable is 4 mm (equivalent to 13 mm full scale).

C. Tabulated Test Results

Table C.1 provides the drag-coefficient results for each yaw angle setting of each run in the test program, with the calculated wind-averaged drag coefficient for each run.

Table C.1: Drag-coefficient measurement results for the SmartWay-verification tests of the NRC Trailer Skirts in the NRC 9 m Wind Tunnel.

Configuration	Run num.	Wind-avg. drag coeff. WAC_D	C_D 0°	C_D -9°	C_D -6°	C_D -3°	C_D -1°	C_D 0°	C_D 1°	C_D 3°	C_D 6°	C_D 9°	C_D 0°
Reference	384	0.5756	0.5267	0.6740	0.6010	0.5406	0.5274	0.5287	0.5306	0.5525	0.6137	0.6832	0.5233
Reference	385	0.5758	0.5275	0.6739	0.6027	0.5397	0.5258	0.5248	0.5301	0.5530	0.6152	0.6811	0.5271
Reference	386	0.5752	0.5253	0.6753	0.6002	0.5413	0.5263	0.5241	0.5288	0.5512	0.6155	0.6804	0.5234
NRC Trailer Skirts	387	0.5188	0.4796	0.5845	0.5375	0.4936	0.4790	0.4785	0.4817	0.5017	0.5449	0.5979	0.4777
NRC Trailer Skirts	388	0.5187	0.4778	0.5833	0.5355	0.4927	0.4776	0.4765	0.4809	0.5030	0.5469	0.5925	0.4783
NRC Trailer Skirts	389	0.5190	0.4775	0.5861	0.5343	0.4922	0.4777	0.4777	0.4804	0.5014	0.5513	0.5970	0.4775
Reference	391	0.5772	0.5257	0.6727	0.6034	0.5427	0.5279	0.5265	0.5325	0.5564	0.6129	0.6837	0.5277

D. Influence of Model Location Over Moving Ground Plane

The moving ground plane is 1 m wide and 5.6 m long, whereas the 30%-scale tractor-trailer model is 6.5 m long. Therefore, the set-up is such that a stationary floor is required under a part of the model. To ensure that the model was positioned appropriately for aerodynamic investigations, in either a forward location with the tractor extending over the stationary floor, or in an aft location with the trailer base and bogie extending over the stationary floor, a shorter 40 ft-equivalent trailer was built for the commissioning process that allowed full coverage of the rolling road under the model. The sleeper-cab with 40 ft trailer configuration was tested with the model in three locations, as shown in Figure D.1, to examine the influence of ground-motion coverage. The drag-coefficient results for these three locations over a range of yaw angles of ±12°are shown in Figure D.2. These results show a negligible change in the drag-coefficient distributions with yaw when moving the model to its forward location. When moving the model to its aft location, a decrease in drag coefficient is observed resulting is a change in wind-averaged drag coefficient of -0.016 (-3%). These results demonstrate that extending the front of the model over the stationary floor is preferable to extending the trailer over the stationary floor. The near-negligible change in wind-averaged drag coefficient with the front of the model exposed to the stationary floor has been attributed to the thin boundary layer ahead of the turntable and moving ground plane, thinned to a displacement thickness of approximately 4 mm by the upstream boundary-layer control system.

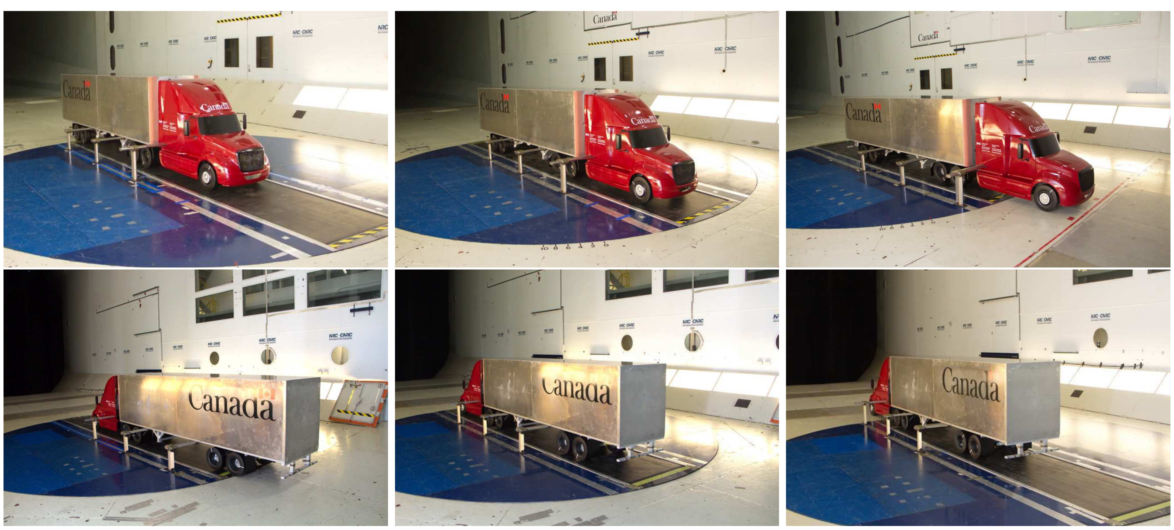

Figure D.1: Sleeper-cab tractor with 40 ft trailer: aft model location (left), mid model location (centre), and forward model location (right).

Surface pressure measurements provide some evidence of where these differences in drag are being generated when the model is moved. Figure D.3 shows the base-pressure distributions for the three locations at 0°yaw angle. No difference is evident between the pressure coeffi-

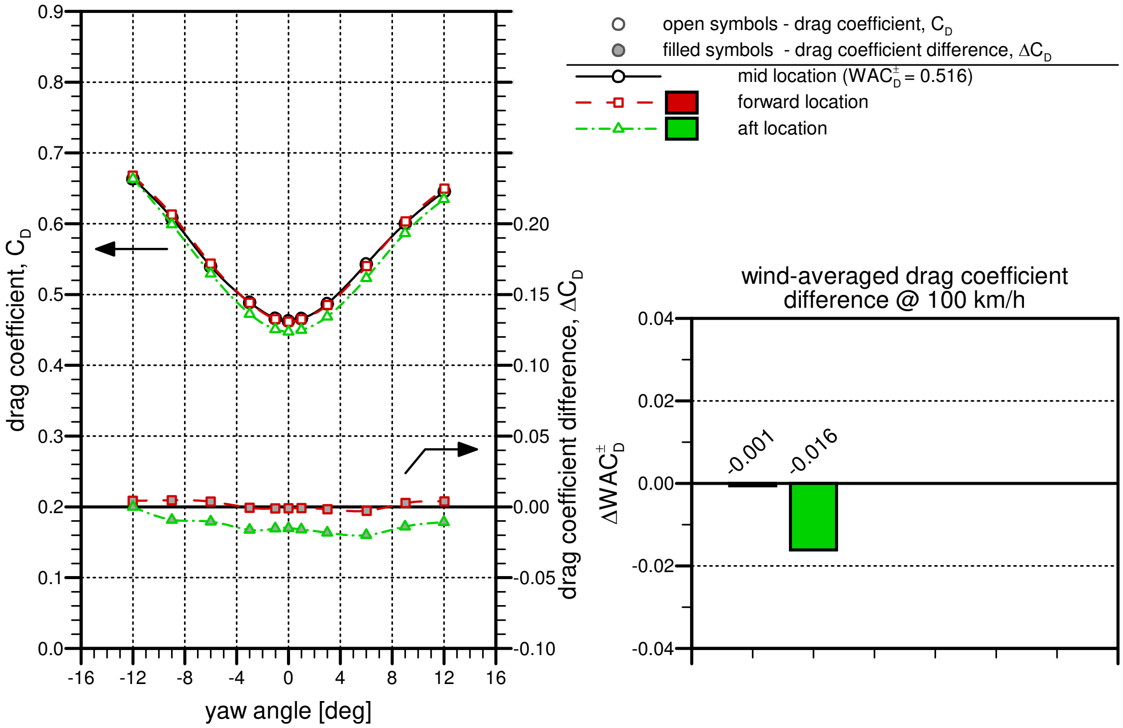

Figure D.2: Influence of model location on the drag-coefficient distributions for the sleeper-cab tractor with the 40 ft dry-van trailer.

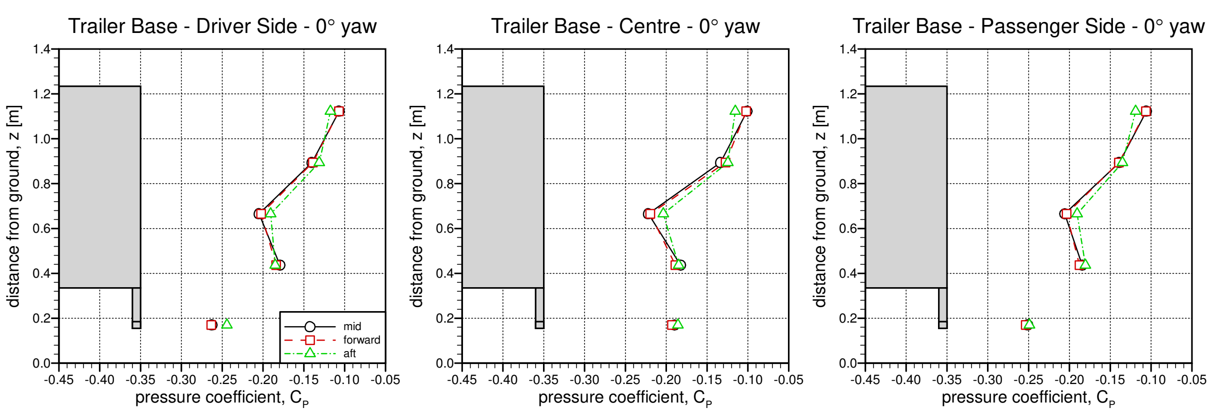

Figure D.3: Influence of model location on the base-pressure-coefficient distributions for the sleeper-cab tractor with the 40 ft dry-van trailer.

cients of the mid and forward locations, with the aft locations showing higher pressures over much of the mid-height region of the trailer base. This higher base pressure reduces the difference in pressures between the front and back of the model, and is likely a major contributor to the reduced drag in this aft-mounted location. These influences are most significant at low yaw angles. The aft location shows no significant differences in the base-pressure patterns be-

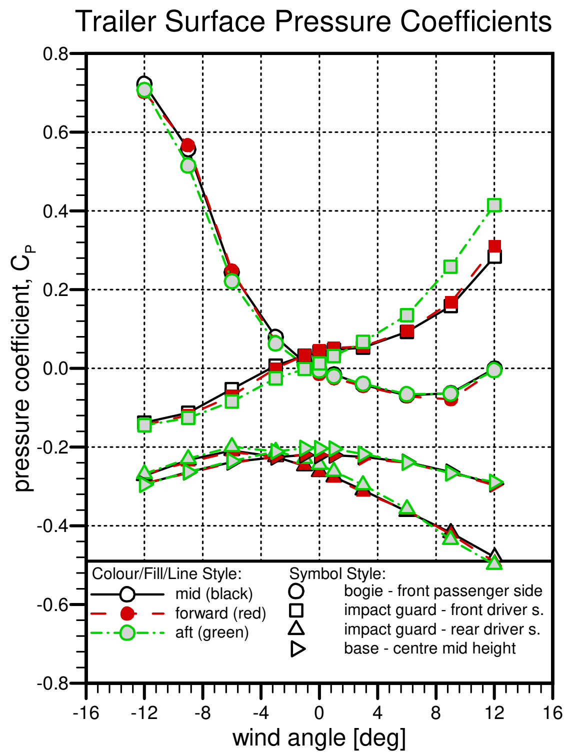

Figure D.4: Influence of model location on select pressure-taps for the sleeper-cab tractor with the 40 ft dry-van trailer.

yond ±3°yaw, as compared to the other locations. Figure D.4, which shows yaw distributions of pressure coefficient for several taps on the trailer, provides additional evidence of where the drag of the vehicle differs with model location. The bogie front face (circle symbols) and rear-impact-guard front driver's-side edge (square symbols) show differences at higher yaw angles that indicate changes to the flow patterns in the trailer bogie and rear under-body region of the model for the aft model location. These changes result from the change in ground-motion boundary conditions which appears to be the the major influence on the vehicle drag at higher yaw angles. This inference of a modified flow pattern in the aft under-body region due to the differences in ground-motion coverage has led to the recommendation that aft under-body and base-mounted devices be tested with the model in its aft position.

E. Recent Modifications to the NCR 30%-Scale Model

The test program documented in the main body of this report was conducted in late 2014. Since that time, modifications have been made to improve the fidelity of the NRC 30%-scale model. In December 2015, the following modifications were made to the model:

- Additional components were added to the engine bay to improve the cooling-drag simulation of the model (see Figure E.1);
- A perforated-plate platform and associated steps were added over the frame rails in the tractor-trailer-gap region (see Figure E.2);
- A drip-rail was added to the upper edge of the trailer roof (see Figure E.3);
- Addition details were added to the trailer base including light enclosures (top and bottom), door hinges, and door latches (see Figure E.4);
- The trailer mudflaps were modified such that they are supported on the trailer bogie instead of the underside of the trailer box (see Figure E.5);
- Treads were added to the wheels (see Figure E.6).

These modifications resulted in an increase of 1% in the wind-averaged-drag coefficient of the model, the majority of which was introduced by the increase in aerodynamic torque on the wheels due to the tire treads.

In November 2016, the following additional modifications will be made to further improve the model fidelity, that may affect the drag performance of the model:

- A seal is being introduced in the cavity between the front grill and the cooling package;
- A mounting frame is being installed behind the bumper and front grill to permit the mounting of devices on the front of the tractor model; and
- Wheel-well fenders are being introduced aft of the tractor steer wheels.

These 2016 modifications have not yet been completed a therefore no photographs are yet available.

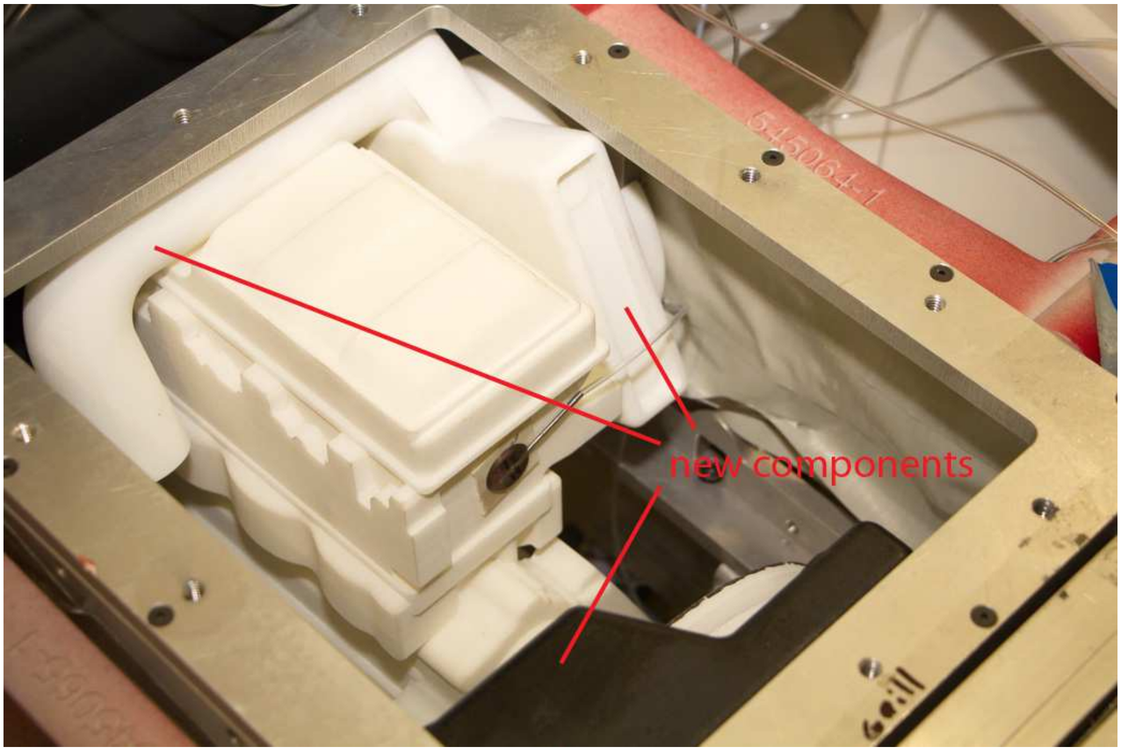

Figure E.1: Model modifications in 2015: engine-bay components.

Figure E.2: Model modifications in 2015: platform and steps.

Figure E.3: Model modifications in 2015: trailer roof-edge drip rail.

Figure E.4: Model modifications in 2015: base details.

Figure E.5: Model modifications in 2015: trailer mud flaps.

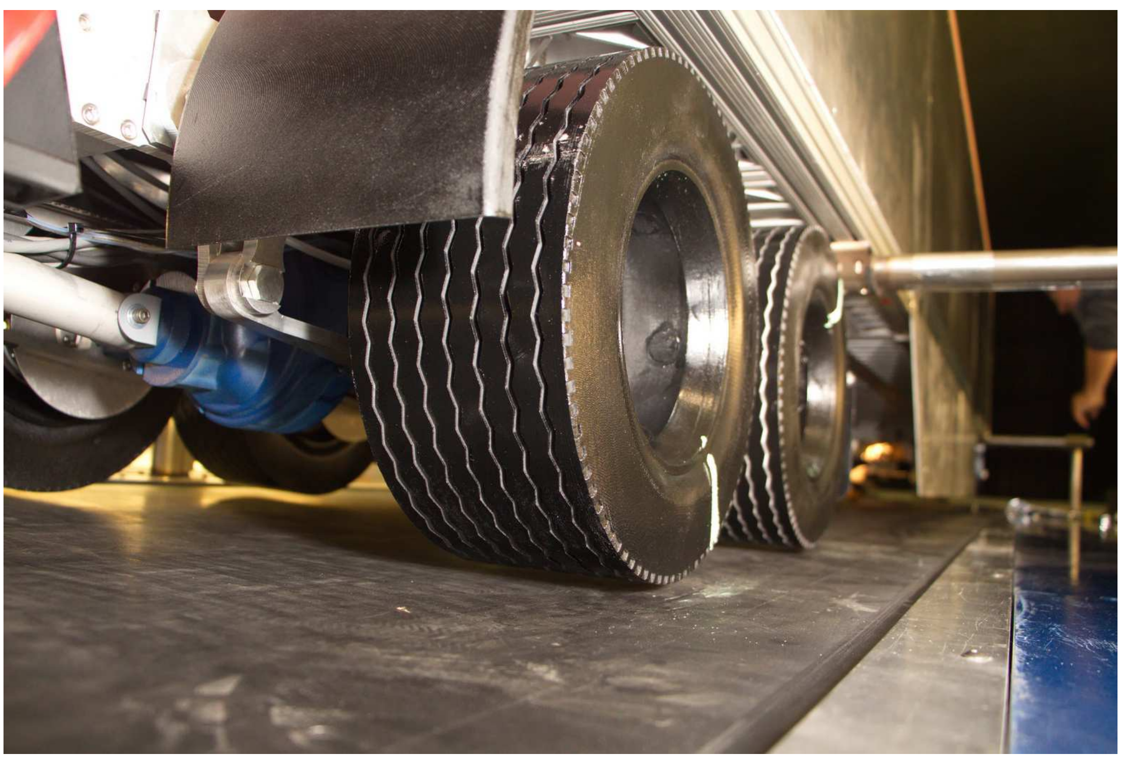

Figure E.6: Model modifications in 2015: wheel treads.